Polymorphism of In5S5Cl, X-ray and HRTEM-Investigations

Hans-Joerg Deiseroth, Vera Nickel, Lorenz Kienle, Viola Duppel, Christof Reiner

Zeitschrift für Anorganische und Allgemeine Chemie

Polymorphism of In5S5Cl, X-ray and HRTEM-Investigations

Journal:	*Zeitschrift für Anorganische und Allgemeine Chemie*
Manuscript ID:	zaac.200900414
Wiley - Manuscript type:	Article
Date Submitted by the Author:	31-Aug-2009
Complete List of Authors:	Deiseroth, Hans-Joerg; Universitaet Siegen, Department of Anorganische Chemie Nickel, Vera; University of Siegen, Chemistry Kienle, Lorenz; University of Kiel, Material Science Duppel, Viola; Max Planck Institute, Chemistry Reiner, Christof; University of Siegen, Chemistry
Keywords:	indium chalcogenide halide, mixed valence, crystal structure, transmission electron microscopy, polymorphism

ARTICLE

DOI: 10.1002/zaac.200((will be filled in by the editorial staff))

Polymorphism of In_5S_5Cl, X-Ray and HRTEM-Investigations

V. Nickel[a], H. J. Deiseroth*, L. Kienle, V. Duppel[b], C. Reiner[c]**

[a] Siegen, Institut für Anorganische Chemie der Universität
[b] Stuttgart, MPI für Festkörperforschung

Dedicated to Prof. Dr. mult. Arndt Simon on the Occasion of his 70th birthday

Keywords: Phase transition; Indium; Electron microscopy; Mixed valence; Chalcogen

Abstract. In_5S_5Cl belongs to the group of mixed valence indium compounds with indium occurring simultaneously in three oxidation states ($In_5S_5Cl = In^+(In_2)^{4+}2In^{3+}5S^{2-}Cl^-$). It was shown in an earlier work that In_5S_5Cl obtained from $InCl_3$, In and S at 550 °C, crystallizes in a monoclinic structure type in contrast to the orthorhombic bromide, In_5S_5Br. The main difference of both structure types is an ordered mutual exchange of In^+ and $(In_2)^{4+}$ in specific crystallographic positions. This exchange is possible due to the almost identical coordination pattern of both ions. A closer inspection of the real structure of monoclinic In_5S_5Cl by High Resolution Transmission Microscopy already showed the presence of small orthorhombic domains in the real structure of this compound. Now we also obtained macroscopic quantities of orthorhombic In_5S_5Cl by the reaction of $InCl_3$, In and S at reaction temperatures below 500 °C ($Pmn2_1$, a = 3.907(1) Å, b = 9.021(2) Å, c = 14.866(3) Å, Z = 2). The new polymorph is analysed by X-Ray single crystal, X-Ray powder and HRTEM investigation.

* Prof. Dr. H.J. Deiseroth
Institut für Anorganische Chemie
Universität Siegen
Adolf Reichwein Strasse 2
D-57076 Siegen
Fax +49 (0)271 7402555
Email: deiseroth@chemie.uni-siegen.de

** Prof. Dr. L. Kienle
Heisenberg-Professur für Synthese und Realstruktur von Feststoffen
Institut für Materialwissenschaften
Technische Fakultät, CAU Kiel
Kaiserstr. 2
24143 Kiel

Introduction

The group 13 element indium forms a great variety of stable mixed valence halides and chalcogenides. Beside the group-specific oxidation numbers +I and +III of the isolated atoms, indium forms cationic clusters of different type with specific average oxidation numbers of the constituting atoms. The most common cluster is an $[In_2]^{4+}$ dumb-bell, occurring in several binary and ternary solids, e.g. in InS [1] or in $KInBr_3$ [2]. Further examples are chain-like $[In_3]^{5+}$- (In_4Se_3, [3]), $[In_5]^{7+}$- and $[In_6]^{8+}$ -units (both in $In_{11}Mo_{40}O_{62}$, [4]), or the tetrahedral $[In_5]^{7+}$ ion, which is observed in $Na_{23}In_5O_{15}$ [5]. All these clusters can be well understood by simple two centre two electron bonds of the constituting atoms. Some of these clusters occur together with In^+ or In^{3+} or simultaneously with both species in the above mentioned mixed valence compounds. A typical example is In_6S_7 ($=In^+(In_2)^{4+}3In^{3+}7S^{2-}$) with Indium in three different oxidation states [6,7]. In such compounds the In-species can be easily distinguished due to their specific coordination and characteristic distances to anions of their first coordination sphere. According to the classification of Robin and Day [8] all these solids belong to group II mixed valence compounds. A peculiar case with respect to this classification is the title compound In_5S_5Cl which contains three different cationic Indium species and two different anionic ones: In_5S_5Cl ($=In^+(In_2)^{4+}2In^{3+}5S^{2-}Cl^-$). In spite of apparent geometrical differences between In^+ and $(In_2)^{4+}$ (In^+: spherical ion, r ≈ 140 pm [9], $(In_2)^{4+}$: dumbbell shaped ion with covalent In-In bonding ($d_{In\text{-}In}$ @ 270 pm [9]) both ions surprisingly have a more or less similar coordination of nine non-metal atoms forming a tri-capped trigonal prism. Due to this peculiar geometrical situation one can expect both ions to be able to interchange their places at least in the sense of a partial disorder. We could show in an earlier work [10] that this is actually possible. A complementary interchange of In^+ and $(In_2)^{4+}$ on specific positions resulting in two different ordered structure types was found for monoclinic In_5Ch_5Cl (Ch = S, Se) "Cl-type" and for orthorhombic In_5Ch_5Br (Ch = S, Se) "Br-type". $TlIn_4Se_5Br$ (with In^+ completely substituted by Tl^+), was the first example to break this initially assumed "systematic" because it crystallizes in the monoclinic "Cl-type" [11]. In_5S_5Cl presented in this paper is the first dimorphic example of this series of solids that forms two polymorphs (monoclinic "Cl type" *and* orthorhombic "Br-type") depending on the synthesis conditions.

Results and Discussion

General remarks

As mentioned above the compounds MIn_4Ch_5X (M = Tl, In, Ch = S, Se, X = Cl, Br) of which $TlIn_4S_5Br$ could not yet been obtained can be described in the mixed valence notation $MIn_4Ch_5X = M^+(In_2)^{4+}2In^{3+}5Ch^{2-}X^-$. The hitherto known compounds crystallize either in the monoclinic "Cl-type" or in the orthorhombic "Br-type". Neglecting the type of non-metals (chalcogen or halogen) the first coordination spheres of the different In/Tl-species are similar in both structure types: octahedral for In^{3+} and tri-capped trigonal prismatic for $(In_2)^{4+}$ and M^+. The octahedra form two-dimensional units of cis- and trans-edge sharing double-octahedra chains extending parallel to the shortest axis of the respective structure type (b for the monoclinic, a for the orthorhombic type) (Fig. 1).

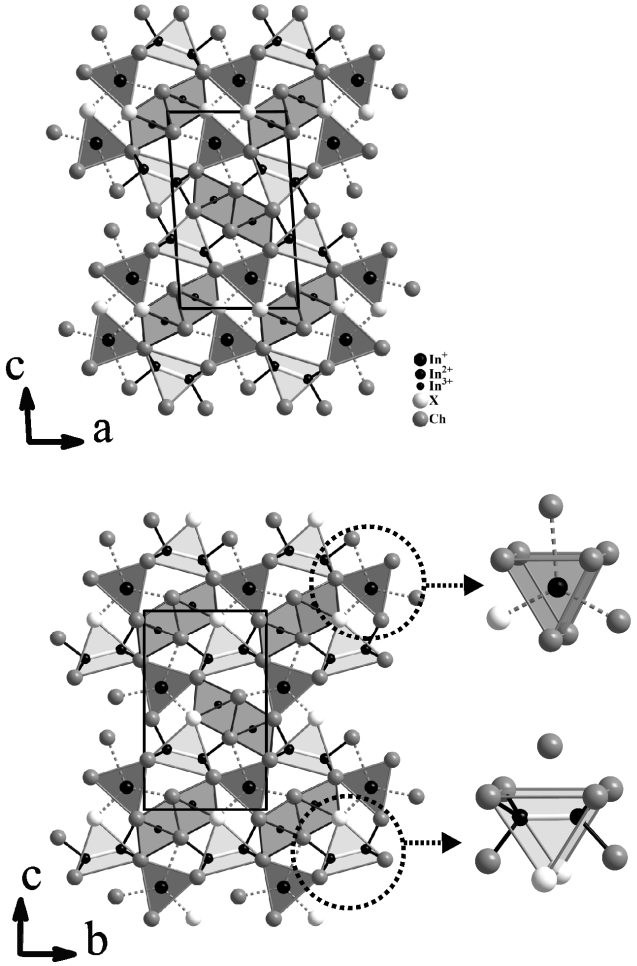

Figure 1: Projection of the monoclinic (above) and orthorhombic (below, left) In_5S_5X (X = Cl, Br) structure type with emphasis on the tri-capped trigonal prismatic coordination of In^+ and $(In_2)^{4+}$ (below right, in projection dark gray or light gray triangles). In the monoclinic type the double octahedra (medium gray) are surrounded either by 4 In^+ and 2 $(In_2)^{4+}$-dumb-bells or by 2 In^+ and 4 $(In_2)^{4+}$-dumb-bells ("4,2" or "2,4"-arrangement). In the orthorhombic type all double octahedra are surrounded by 3 In^+ and 3 $(In_2)^{4+}$-dumb-bells ("3,3"-arrangement).

Both structure types can be easily distinguished in structure projections along the short axis focusing on the local pattern formed by the $In(Ch/X)_6$-octahedra and the surrounding trigonal prisms as outlined in detail in [10] and summarized in Figure 1. In an earlier work we could show by HRTEM investigations that the real structure of orthorhombic In_5S_5Br on an atomic scale is nearly free of chemical defects, while the *monoclinic* In_5S_5Cl exhibits *multiple twinning*, an *intergrowth* with In_6S_7 in nano-dimensions and thin, in rare cases more expanded *lamellar intergrowth* of *orthorhombic* In_5S_5Cl [10], which was not yet known as macroscopic phase at that time. Earlier experiments to enhance the size of the orthorhombic domains in In_5S_5Cl by annealing "monoclinic" In_5S_5Cl at different temperatures failed. In the course of a series of further synthesis experiments in the system indium-sulphur-chlorine at lower temperatures we now obtained surprisingly orthorhombic In_5S_5Cl in macroscopic quantities.

X-Ray powder Investigations of monoclinic and orthorhombic In_5S_5Cl-samples

Monoclinic In_5S_5Cl can be obtained from mixtures of $InCl_3$, In and S with the total composition In_5S_5Cl which are annealed *above* 500 °C (e.g. 550 °C). The product consists of extremely thin (1-15 µm) orange-red transparent needles with a length up to some mm. Scanning electron images show that these needles typically are bundles of several crystals with intergrowth along the needle axis [010]. X-Ray powder patterns of such samples in comparison to calculated patterns based on single crystal data show a good agreement concerning the positions of the reflection angles. Strong differences of intensities [10] are due to texture effects, which result from a preferred orientation of the needles on a flatbed holder or in a capillary. A careful inspection of the resulting powder diagrams gives no evidence for the presence of additional orthorhombic In_5S_5Cl.

From mixtures of $InCl_3$, In and S with the total composition In_5S_5Cl which are annealed *below* 500 °C the new orthorhombic modification of In_5S_5Cl is formed. Orthorhombic In_5S_5Cl can already be detected by powder X-ray diffraction in samples which were annealed at 300 °C only. The visible formation of needles, however, becomes more pronounced with increasing temperature. At a higher magnification and with a certain experience the needles of orthorhombic In_5S_5Cl can even be distinguished from the monoclinic ones. The latter ones show a more regular shape and less intergrowth along the needle axis. X-ray powder patterns exhibit only minor texture effects. Measured and calculated patterns agree almost completely (Figure 2 (a)). In particular no reflections of the monoclinic modification of In_5S_5Cl are present (Figure 2 (b)). Samples of orthorhombic In_5S_5Cl which are annealed at 550°C show new reflections of the monoclinic polymorph already within one day. After five days the transition is complete. We assume that the sample recrystallizes under participation of a gas phase reaction including molecular species like In_2Ch and InX. An alternative interdiffusion of $(In_2)^{4+}$ and In^+ ions in the bulk seems unlikely. It is *not* possible to transform monoclinic In_5S_5Cl back to the orthorhombic polymorph by annealing the monoclinic phase *below* 500 °C. This behaviour was checked at several temperatures in the range of 300-500°C and with different annealing times (up to 4 weeks). The volumes of the two polymorphs which result from the refinements of X-ray powder patterns show only minor differences (Table 1). In Differential Thermal Analyses both polymorphs exhibit a thermal effect in the

same temperature range (590 °C for orthorhombic and 605°C for monoclinic In_5S_5Cl).

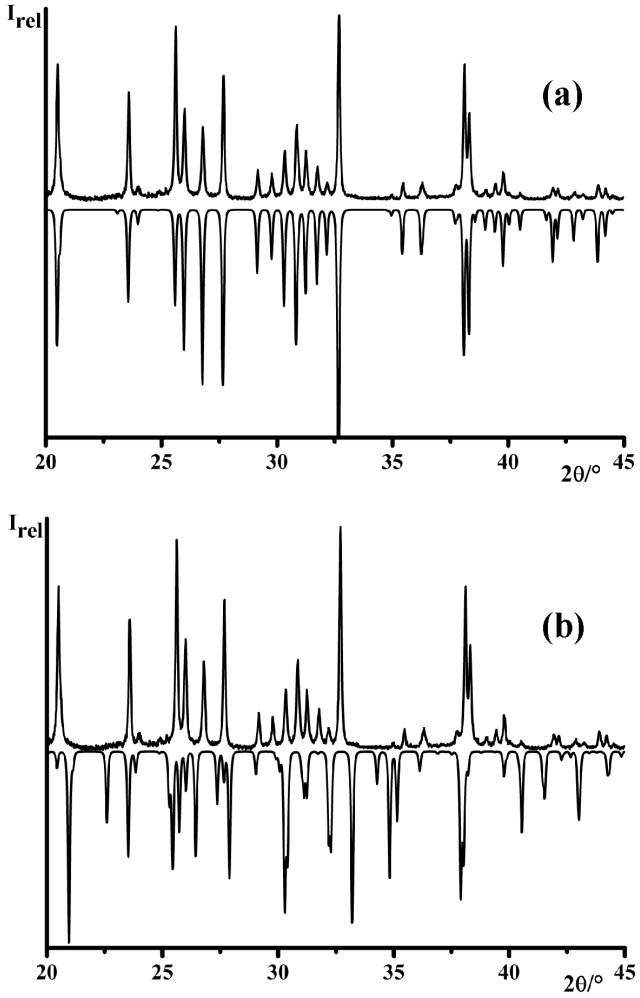

Figure 2: (**a**) Section of a measured X-Ray powder pattern of orthorhombic In_5S_5Cl (above) in comparison to a calculated one (below, calculated from single crystal data). (**b**) Sections of a measured X-Ray powder pattern of orthorhombic In_5S_5Cl (above) in comparison to a calculated one of monoclinic In_5S_5Cl (below, calculated from single crystal data) [10].

Table 1 Comparison of the lattice constants for the monoclinic and orthorhombic polymorphs of In_5S_5Cl obtained from powder data with internal standard (Si).

	Lattice constants /Å / ° /Å^3	**Space group**
In_5S_5Cl	a = 8.944(2), b = 3.9111(8), c = 14.985(4), β = 93.60(3) V = 523.1(2)	$P2_1/m$
In_5S_5Cl	a = 3.9031(1), b = 9.010(3), c = 14.836(5), V = 521.7(2)	$Pmn2_1$

Powder investigations of samples which are quenched from temperatures slightly above these thermal effects prove that these temperatures represent in both cases the decomposition of the solids.

X-Ray single crystal investigation and comparison of the polymorphs

For a single crystal measurement a small reddish transparent needle of orthorhombic In_5S_5Cl was selected from a heterogeneous sample which was annealed at 550 °C for one day only (see above). The crystal was measured on a STOE IPDS I. The analyse of the collected data with the programs RECIPE and SPACE [12] showed the presence of three domains which were intergrown unsystematically. With the program TWIN [12] overlapping reflections were rejected and the data of the major domain were used for the structure solution and refinement. A summary of the data collection, refinement details and atomic positions is given in tables 2 and 3.

Table 2 Summary of data collection and refinement details for orthorhombic In_5S_5Cl.

Sum formula	In_5S_5Cl
Formula weight /g mol^{-1}	769.85
Space group	$Pmn2_1$
Formula units per unit cell	Z=2
Crystal shape	dark-red needle
Crystal dimension /mm^3	0.1 x 0.02 x 0.01
lattice constants /Å /°	a = 3.907(1)
	b = 9.021(2)
	c = 14.866(3)
Volume /Å^3	V = 524.0(2)
Density (calc.) / g cm^{-3}	ρ = 4.880
Absorption coefficient /mm^{-1}	μ = 12.019
F (000)	684
Diffractometer	STOE-IPDS
	(Graphite monochromator)
Wavelength /Å	0.71073 (Mo-Kα)
Temperature /K	T = 293
Measured θ range /°	2.64 - 29.22
Index ranges	$-5 \geq h \geq 4$, $-12 \geq k \geq 12$, $-20 \geq l \geq 20$
Measured reflections	1560
Independent reflections	1380
Completeness to θ /%	96.6
$R_{int.}$	0.0652
Data/Restraints/Parameter	1560 / 1 / 69
R values (I≥2σ(I))	R_1 = 0.0335, wR_2 = 0.0719
R values (all data)	R_1 = 0.0421, wR_2 = 0.0749
Weighting scheme*	A = 0.0458 B = 0
GooF	0.976
Difference Fourier	$\rho_{max.}$ = 1.782
residuals /e Å^{-3}	$\rho_{min.}$ = -1.222

* $w=1/[\sigma^2(F_0^2) + (AP)^2 + BP]$, $P=(F_0^2) + 2F_c^2)/3$

In contrast to monoclinic In_5S_5Cl the structure refinement of orthorhombic In_5S_5Cl does not show any significant anomalies. This is somewhat surprising because In_5S_5Cl is the first dimorphic example thus exhibiting ideal requirements for a nanoscale intergrowth of both modifications. In order to ensure this observation and to derive information about the homogeneity on a nanoscale, HRTEM investigations were carried out (see below).

Table 3 Atomic coordinates, equivalent isotropic displacement parameters U_{eq} /Å^2 and occupancy for orthorhombic In_5S_5Cl, all atoms in Wyckoff position 2*a*.

Atom	*x*	*y*	*z*	U_{eq} [Å^2]	sof
In1	0	0.8876(1)	0.40427(6)	0.0119(2)	1
In2	1/2	0.5990(1)	0.52420(6)	0.0120(2)	1
In3	1/2	0.1880(1)	0.30337(7)	0.0161(2)	1
In4	1/2	0.48008(9)	0.25427(6)	0.0115(2)	1

In5	1/2	0.8579(2)	0.11078(8)	0.0283(4)	0.951(6)
S1	1/2	0.7001(3)	0.3615(2)	0.0084(6)	1
S2	1/2	0.4290(3)	0.6604(2)	0.0104(6)	1
S3	0	0.7674(3)	0.5658(2)	0.0096(6)	1
S4	1/2	0.0642(4)	0.4556(2)	0.0119(6)	1
S5	0	0.0296(3)	0.2518(2)	0.0122(5)	1
Cl	0	0.4096(3)	0.4593(2)	0.0153(6)	1

Table 4 Comparison of selected distances /Å for monoclinic [10] and orthorhombic In_5S_5Cl.

In_5S_5Cl, monoclinic			In_5S_5Cl, orthorhombic		
In1-	S5	2.57(1)	In1-	S5	2.603(3)
	S2(2x)	2.620(7)		S4(2x)	2.634(2)
	S1	2.61(1)		S3	2.634(3)
	S1(2x)	2.653(7)		S1(2x)	2.661(2)
	Ø	2.621		Ø	2.638
In2-	S3	2.54(1)	In2-	S3(2x)	2.551(2)
	S4(2x)	2.544(7)		S2	2.540(3)
	S4	2.59(1)		S1	2.585(3)
	Cl(2x)	2.776(7)		Cl(2x)	2.769(2)
	Ø	2.628		Ø	2.628
In3-	S2	2.50(1)	In3-	S4	2.524(3)
	S5(2x)	2.57(1)		S5(2x)	2.539(2)
	Ø	2.547		Ø	2.534
In4-	S3(2x)	2.517(7)	In4-	S2(2x)	2.537(2)
	S1	2.54(1)		S1	2.546(3)
	Ø	2.527		Ø	2.540
In4-	In3	2.723(4)	In4-	In3	2.734(1)
In5-	Cl(2x)	3.187(9)	In5-	S4(2x)	3.103(3)
	S5(2x)	3.206(9)		S5(2x)	3.257(3)
	S4	3.28(1)		Cl	3.301(3)
	Cl	3.34(1)		S2(2x)	3.326(3)
	S3(2x)	3.398(9)		S3	3.446(3)
	S1	3.93(1)		S1	3.990(3)
	Ø	3.348		Ø	3.345

As mentioned above the crystallographically independent In atoms have the same type of coordination in both polymorphs (Figure 1). The average and individual In-Ch/X distances are reasonable and show good internal and external agreement (Table 3). Nevertheless a significant difference in the first coordination sphere is observed for In5 (In^+). In the monoclinic phase the first coordination sphere of In5 consists of six S and three Cl atoms while in the orthorhombic polymorph In5 has eight S and one Cl atom. All other In atoms have the same ratio S/Cl in their coordination sphere. The slight under-occupancy for In5 (In^+) is a feature of all solids containing In^+. It is most likely due to an interchange of a small fraction of In^+ and $(In_2)^{4+}$.
The Madelung Parts of Lattice Energy (MAPLE, [13,14]) for monoclinic and orthorhombic In_5S_5Cl favors the monoclinic phase over the new orthorhombic one($\Delta \approx 0.8$ %, Table 5). The partial MAPLE values of the octahedrally coordinated In^{3+} (In1 and In2) are more balanced for the monoclinic compound. The small value for Cl^- in the monoclinic phase is remarkable. In both structure types three of five crystallographically independent chalcogen atoms have significant higher values than two others. For the evaluation of this calculation one should consider, that only the orthorhombic structure type does *not* show chemical defects (see below).

Table 5 MAPLE values for monoclinic [10] and orthorhombic In_5S_5Cl.

	MAPLE /kcal/mol monoclinic	MAPLE /kcal/mol orthorhombic
In1 (In^{3+})	-873,53	-911,63
In2 (In^{3+})	-831,28	-808,78
In3 (In^{2+})	-328,12	-337,65
In4 (In^{2+})	-341,63	-318,64
In5 (In^+)	-149,57	-159,44
S1	-442,47	-463,59
S2	-473,40	-413,13
S3	-395,47	-443,57
S4	-461,87	-378,02
S5	-386,62	-368,18
Cl1	-78,44	-124,13
Σ	**-4762,4**	**-4726,76**

HRTEM investigations of orthorhombic In_5S_5Cl

The crystal structure of the chemically homogeneous samples was examined via electron diffraction techniques. All analyzed selected areas (about 50) show Bragg intensities which can be indexed assuming the orthorhombic structure type. Particularly for zone axis [100] which correlates with the [010] orientation of the monoclinic structure exactly rectangular patterns were recorded. This contrasts to monoclinic In_5S_5Cl which exhibits significant deviations from rectangularity and orthorhombic symmetry. Diffuse scattering, particularly diffuse streaks 00l indicating lamellar intergrowth phenomena was *not* observed. Strongly excited but kinematically forbidden reflections directed our attention to structural deviations from the orthorhombic model with space group $Pmn2_1$. A careful comparison of different electron diffraction techniques led to the conclusion that such violations (which are *not* observed in the X-Ray experiments) are produced by multiple scattering effects. The intensity of the kinematically forbidden reflections is strongly minimized when tilting the crystal from the precise zone axis orientation or when applying precession electron diffraction. In this case an average of many tilted patterns is recovered by moving the electron beam on a precession cone [15]. One example is presented in Figure 3 for a thick crystal along [110]. The serial reflection condition (00l with l = 2n) is strongly violated in the SAED pattern which was performed with a fixed electron beam (a), cf. arrows. These intensities are strongly reduced when switching to the precession mode (c). Moreover, the expected differences in reflection intensity are more pronounced in the PED pattern and approximate well the simulated pattern of b).

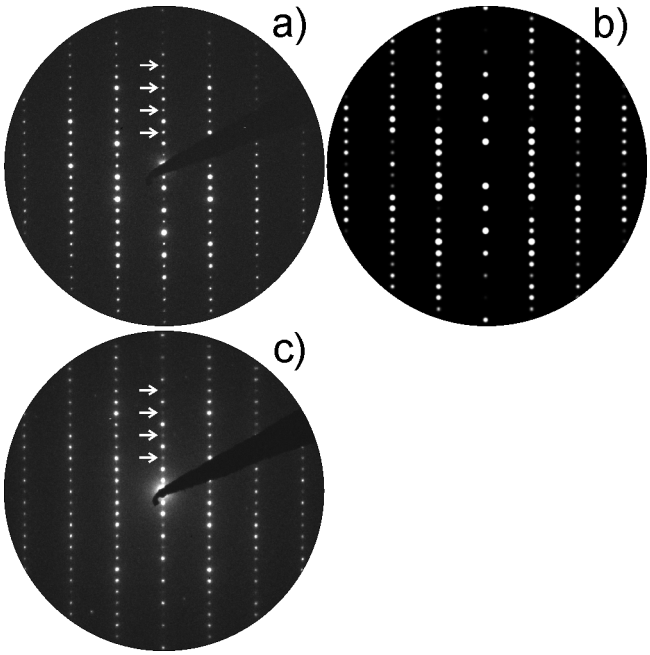

Figure 3 a) SAED pattern, b) simulated PED pattern (precession angle 3°, thickness: 20 nm), c) PED pattern. All zone axis [110].

The absence of stripes in bright-field contrast, the HRTEM micrographs and the corresponding Fourier transforms proof that lamellar structures based on chemical, or polymorphic intergrowth and twinning as described for the sample annealed at 550 °C [10] were limited to exceptional cases. The single layers are imaged edge-on in all zone axes orientations [*uv*0], e. g. [100]. As specified above only one type of layer is present for the orthorhombic structure type, and adjacent layers appear shifted and inversed when projected along [100]. Consequently, the characteristic contrasts representing the layers are shifted and inversed as well, cf. Figure 4. The cut-out in a) left shows the contrast simulation for a single layer (Δf = -40 nm) based on the model from X-ray analysis. On the right four of these cut-outs are combined by applying a shift and an inversion like for the consecutive layers in the orthorhombic structure. The experimental micrograph (Figure 4b)) clearly shows the arrangement of the layers and the good correlation to the inserted simulation proofs the 3,3-arrangement of the single layers. A convincing agreement of simulated and experimental micrographs is also found when varying the focus, e. g. when selecting strong underfocus conditions, cf. Figure 4 c).

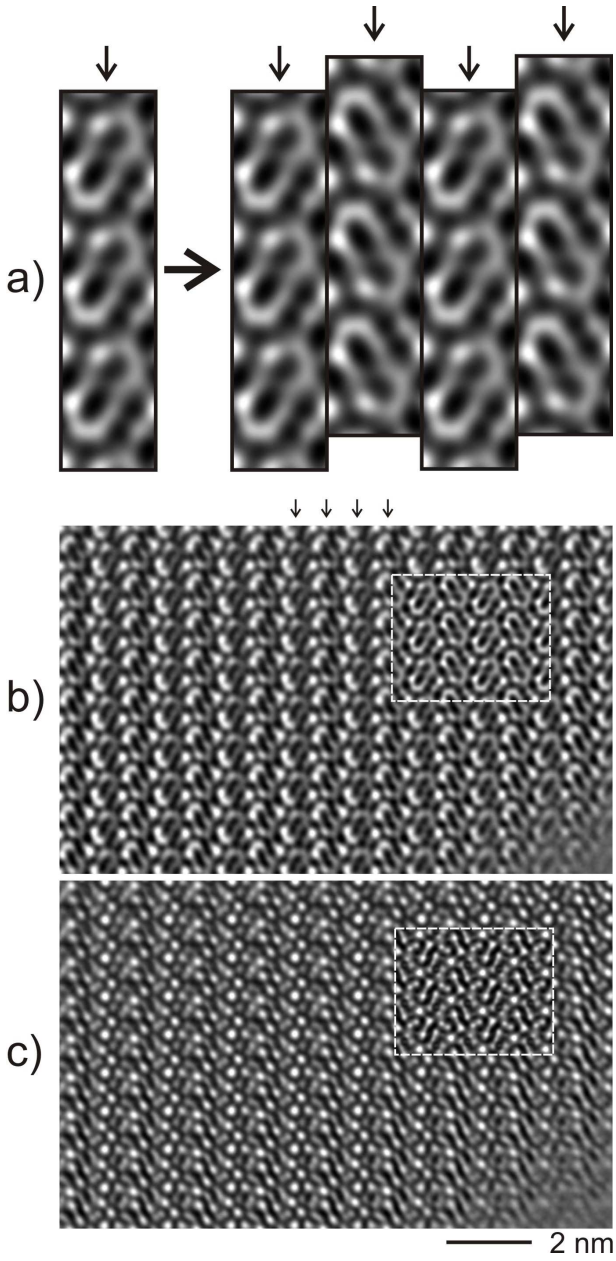

Figure 4 a) Cut-out of a simulated micrograph based on ortho-rhombic In_5S_5Cl and composite image, see text; b) and c) experimental micrographs and inserted simulations with Δf = -40 nm and Δf = -85 nm, respectively (t = 3.9 nm). All zone axis [100], the images of a) were scaled by 300 % with respect to b) and c).

Experimental Section

Synthesis. The synthesis of the polymorphs of In_5S_5Cl was carried out from sulphur (Chempur, pieces, 99,999%), indium (Chempur, shots, 99,9999%) and $InCl_3$ (Heraeus, powder, 99,999%) in stoichiometric amounts (ratio 14:15:1) or from the powdered binary educts InS (prereacted from In and S), In_2S_3 (Alfa, powder, 99,999%) and $InCl_3$ in the ratio 2:1:1. The respective educts were weighed in an Ar-filled glove box and transferred into evacuated dry quartz glass ampoules (d = 12 mm, l = 60-80 mm). The samples were heated to the final temperature and annealed for several days or weeks.

For temperatures above 723 K fine needle-shaped crystals of monoclinic In_5S_5Cl were observed. The crystals are dark-red and not markedly air sensitive. For temperatures between 573 K and

723 K the resulting reddish-brown powder consists of microcrystalline, orthorhombic In_5S_5Cl. Below an annealing temperature of 573 K no In_5S_5Cl is formed. The annealing of a homogenised orthorhombic microcrystalline phase for one day at 723 K leads to a partial transformation to the monoclinic phase. Simultaneously monoclinic and orthorhombic needle shaped crystals suitable for single crystal analyses are formed.

X-Ray Powder investigations. X-Ray powder measurements were carried out on a SIEMENS D5000 diffractometer (transmission mode) with Ge-monochromatized Cu-Kα_1 radiation. To verify the lattice constants of the two modifications of In_5S_5Cl, X-Ray powder diagrams were measured with an internal standard (silicon).

X-Ray single crystal investigation. For X-Ray structure determination of orthorhombic In_5S_5Cl a needle-shaped crystal with appropriate size was separated from the bulk, fixed with grease on top of a glass capillary and mounted on a STOE IPDS I imaging plate diffraction system using graphite monochromatized Mo-Kα radiation. Data analysis and evaluation were done by the STOE IPDS program package [12]. The programs RECIPE [12] and SPACE [12] were used to analyze the reciprocal space. For structure solution SHELXS97 [16] was used. The structure was refined as an inversion twin using SHELXL97 [17].
A summary of crystal and experimental data as well as structure refinement details for orthorhombic In_5S_5Cl is reported in Table 2-3. Further details of the crystal structure investigation are available from the Fachinformationszentrum Karlsruhe, D-76344 Eggenstein-Leopoldshafen (Germany), on quoting the depository number CSD-xxxxxx, the name of the author(s) and citation of the paper.

Thermal analysis. Differential thermal analysis was carried out on a LINSEIS L-62 instrument. Carefully ground samples (sealed in evacuated quartz glass capillaries) were heated to a final temperature of 1073 K with heating/cooling rates of 5 K/min. Orthorhombic In_5S_5Cl shows two endothermic effects upon the heating cycle, one at 856 K, and a second broader one at 966 K. After heating up the sample to 860 K followed by rapid cooling (fast lifting of the DTA-oven, estimated cooling rate 573 K/min), the resulting powder diagrams showed the presence of In_6S_7 as a decomposition product and reflections of orthorhombic In_5S_5Cl.

HRTEM.
All specimens were placed on copper grids which were fixed in a side-entry, double-tilt holder with the tilting limited to a maximum of ± 25° in two directions. High resolution transmission electron microscopy (HRTEM), precession electron diffraction (PED) and selected area electron diffraction (SAED) were performed in a Philips CM30ST (300 kV, LaB_6 cathode). The EMS program package [18] was applied for the simulation of HRTEM micrographs and electron diffraction patterns. EDX (energy dispersive X-ray spectroscopy) was performed in the scanning- and nanoprobe mode of CM30ST with a Si/Li-EDX detector (Noran, Vantage System).

Acknowledgments

The authors would like to thank the *Deutsche Forschungsgemeinschaft* for continuous financial support

Received: ((will be filled in by the editorial staff))
Published online: ((will be filled in by the editorial staff))

[1] R. Walther, H. J. Deiseroth, *Z. Kristallogr.* **1995**, *210*, 360-360.

[2] G. Meyer, T. Staffel, R. Dronskowski, M. Scholten, *Z. Anorg. Allg.* **1998**, *624*, 1741-1745.

[3] J. H. C. Hogg, H. H. Sutherland, *Acta Crystallogr.* **1973**, *B29*, 1590-1593.

[4] E. M. Peters, A. Simon, H. Mattausch, *Inorg. Chem.* **1986**, *25*, 3428-3433.

[5] H. J. Deiseroth, H. Kerber, R. Hoppe, *Z. Anorg. Allg.* **1998**, *624*, 541-549:

[6] H. J. Deiseroth, H. Pfeifer, A. Stupperich, *Z. Kristallogr.* **1993**, *207*, 45-52.

[7] J. H. C. Hogg, W. J. Duffin, *Acta Crystallogr.* **1967**, *A23*, 111-118.

[8] M. B. Robin, P. Day, *Adv. Inorg. Chem. Radiochem.* **1967**, *10*, 247-403.

[9] C. Reiner, PhD thesis, **1998**, University of Siegen.

[10] H. J. Deiseroth, C. Reiner, K. Xhaxhiu, M. Schlosser, L. Kienle, *Z. Anorg. Allg. Chem.* **2004**, *630*, 2319-2328.

[11] V. Nickel, C. Reiner, M. Schlosser, H. J. Deiseroth, L. Kienle, K. Xhaxhiu, *Z. Anorg. Allg. Chem.* **2004**, *634*, 2209-2216.

[12] STOE & CIE, IPDS-Software, Version 2.93, Darmstadt, **1999**.

[13] R. Hoppe, R. Hübenthal, *MAPLE 4* Program for the calculation of MAPLE values, University of Gießen, **1993**.

[14] R. Hoppe, *Angew. Chem. Int. Ed.* **1966**, *5*, 95-106.

[15] a) R. Vincent, P. A. Midgley, *Ultramicroscopy* **1994**, *53*, 271-282; b) J. Gjonnes, V. Hansen, A. Krerneland, *Microsc. Microanal.* **2004,** *10*, 16-20; c) T. E. Weirich, J. Portillo, G. Cox, H. Hibst, S. Nicolopoulos, *Ultramicroscopy* **2006**, *106*, 164-175; d) M. Gemmi, X. Zou, S. Hovmoller, A. Migliori, M. Vennstrom, Y. Andersson, *Acta Crystallogr.* **2003**, *A59*, 117-126; e) C. Own PhD thesis, Northwestern University Evanston Illinois December **2005**.

[16] G.M. Sheldrick, SHELXS-97 Program for the Solution of Crystal Structures, Universität Göttingen, **1997**.

[17] G.M. Sheldrick, SHELXL-97 Program for the Refinement of Crystal Structures, Universität Göttingen, **1997**.

[18] Stadelmann P. A., *Ultramicroscopy* **1987,** *21*, 131-148.